

Journal of Materials Chemistry B

Accepted Manuscript



This is an *Accepted Manuscript*, which has been through the Royal Society of Chemistry peer review process and has been accepted for publication.

Accepted Manuscripts are published online shortly after acceptance, before technical editing, formatting and proof reading. Using this free service, authors can make their results available to the community, in citable form, before we publish the edited article. We will replace this *Accepted Manuscript* with the edited and formatted *Advance Article* as soon as it is available.

You can find more information about *Accepted Manuscripts* in the [Information for Authors](#).

Please note that technical editing may introduce minor changes to the text and/or graphics, which may alter content. The journal's standard [Terms & Conditions](#) and the [Ethical guidelines](#) still apply. In no event shall the Royal Society of Chemistry be held responsible for any errors or omissions in this *Accepted Manuscript* or any consequences arising from the use of any information it contains.

Anti-IgG-anchored liquid crystal microdroplets for label free detection of IgG

Kyubae Lee^a, Kailash Chandra Gupta^{a,b}, Soo-Young Park^a and Inn-Kyu Kang^{a,*}

^aDepartment of Polymer Science and Engineering, Kyungpook National University, Daegu 702-701 Republic of Korea

^bPolymer Research Laboratory, Department of Chemistry, I.I.T. Roorkee-247667 India

Abstract

The orientational variation of 4-cyano-4'-pentyl biphenyl (5CB) molecules in LC microdroplets in response to IgG antigen (IgG) interactions has been utilized to develop a biosensor for rapid and label-free detection of IgG in biological fluids. In order to prepare a LC microdroplet-based biosensor, the anti-IgG (AIgG) anchored 4-cyano-4'-pentyl biphenyl LC microdroplets were prepared in presence of sodium dodecylsulfate (SDS) as mediator and amphiphilic poly (styrene-*b*-acrylic acid) (PS-*b*-PA) as modifier of LC/water interface. The AIgG-anchored LC microdroplets with a size variation from 20 to 30 μm have been used successfully for the detection of IgG within a concentration range of 20 to 1000 ng/mL, at a detection limit of as low as 16 ng/mL, and a response time of 30 min in PBS solution at room temperature. The LC microdroplets anchored with 5 $\mu\text{g/mL}$ of AIgG found to be more sensitive for the detection of IgG in concentration range from 20 to 800 ng/mL in PBS. The AIgG-anchored LC microdroplets have shown a delayed response of 90 minutes for IgG in a solution containing 10% FBS or 10% blood plasma in comparison to PBS solution. The LC microdroplets anchored with 5 $\mu\text{g/mL}$ (34 pmol) of AIgG have shown a recovery of 106% of IgG, coefficient of variance of $\pm 4\%$ and precision within a limit of 1-6% for a spiked sample of 25 ng/mL of IgG. The results indicated that orientational response of LC microdroplets is potentially useful to develop a biosensor for *in vivo* detection of proteins or pathogens in a biological fluid.

1. Introduction

The protein level in blood serum provides a direct basis to assess the state of disease in a patient. Therefore, blood serum proteins considered attractive targets to develop sensors for the detection and diagnostic applications of diseases. The simple and sensitive immunoassaying of disease antigens in homogeneous liquid conditions using label-free techniques potentially eliminates the need for traditional cumbersome microscopic methods,¹ which require skilled personnel and sufficient time for preparation of samples for analysis. Therefore, there is a need to develop a rapid and cost-effective diagnostic method for the sensitive detection of disease-causing antigens in infected blood samples. The conventional enzyme-linked immunosorbent assaying (ELISA) method is time consuming for immunoassaying of proteins in the blood and feasible on interaction of immunoreagent on contacting surfaces.² At present, owing to the high specificity and strong affinity of antibodies for disease-causing antigens, immunoassaying using antibody–antigen interactions is the preferred tool for detection of nanomolar amounts of antigen in the blood samples.³ The activity of gold nanoparticle (AuNP)–antibody conjugates in detection of antigen has been shown to be dependent on the method of conjugation of the antibody.^{2,4} A number of immunoassaying methods, such as fluorescence polarization,⁵ fluorescence resonance energy transfer (FRET),³ bioluminescence resonance energy transfer,⁶ surface plasmon resonance,⁷ and light scattering,⁸ have been used for the detection of proteins in blood samples. However, most of these homogeneous protein assaying methods have been found to be less sensitive and expensive in comparison to other methods such as ELISA and dot-blot immune method.⁹ Most antibody-anchored nanoparticle-based sensitive immunoassaying methods used for the detection of antigen, SKBR-3 breast cancer cells,¹⁰⁻¹⁵ and bacteria^{16,17} require the extraction of antigen from cells for the immunoassay to be performed. This introduces

difficulties in assaying antigens precisely, as these methods involve several steps for immunoassaying of antigen in biological matrices. The enhanced fluorescence technique has also been used in immunoassaying *Escherichia coli* strain O157 using antigen-coated silica nanoparticles.¹⁸ Recently, aptamer–bacterial protein interactions have been exploited for the detection of bacteria utilizing aptamer-coated CdSe/ZnS quantum dots.¹⁹ Upconversion nanoparticles (UCNs) conjugated with anti-HER2 antibody have been successfully utilized for the detection of the fluorescent HER2 receptors of SKBR-3 breast cancer cells.²⁰ The antibody-immobilized microchip of an electrochemical immunoassay system was found to be able to detect prostate-specific antigen in human serum with 75% accuracy.²¹ However, fluorescent green protein-nanoparticle conjugates were found to be able to simultaneously detect five serum proteins with 100% success in buffer, and 97% success in human serum.²² The long range orientation order of LC molecules has been used successfully to develop biosensors for the detection of P53 mutation gene within the concentration range from 0.08-8 nM.²³ The conformational changes in oligonucleotides on interactions with heavy metal ions have been used to develop a LC based biosensor for label free detection of Hg²⁺ ions with a lower limit of detection (LOD) of 0.1nM.²⁴ To enhance the sensitivity in detection of analytes, the signal enhanced LC DNA biosensor has been developed using enzymatic silver deposition method.²⁵ These studies clearly indicate that antibody-conjugated LC based biosensors may be developed for the detection of disease causing proteins and cancer-specific antigens. The liquid crystal microdroplets based biosensor for the detection of antigens is not reported in the literature. However, LC microdroplets based sensors have been used in detection of interfacial events involving interactions between chemicals²⁶⁻³¹ and viruses.³² In some other studies, LC signal based systems have been used for the detection of proteins on solid surfaces³³⁻³⁶ and LC–water

interfaces.³⁷⁻³⁹ Unlike AuNP-based immunoassaying of proteins, LC signal based detection systems do not require fluorescent labeling as the orientational response in LC molecules is utilized as the basis for detection of antibody-protein interactions at the interface. The LC-based sensing systems have been simplified by using LC molecules as small droplets, which found to be potentially more sensitive⁴⁰⁻⁴⁶ in comparison LC molecules used for sensing on solid surfaces.³³⁻³⁶ The high sensitivity of LC microdroplets is attributed to their small size, mobility, and high surface area in comparison to solid-surface LC systems.⁴⁷⁻⁴⁸ The interfacial area of LC molecules in the form of microdroplets is comparatively more than the same amount of LC molecules placed on confined planar surfaces. The LC droplets have well defined director with tunable optical properties.⁴⁹⁻⁵¹ The interaction forces between LC microdroplets and species are sufficiently enough to produce detectable optical signal in presence of small amount of species at the interface. The sensitivity of LC molecules on planar solid surfaces is limited as interactions forces are not sufficient to cause detectable optical transitions in LC molecules in presence of small amount of analytes at the interface. Recently, a microfluidic device-based LC system is developed for naked eye detection of antibody with a lower limit of detection of $1\mu\text{g/mL}$,⁵² which supported the enhanced sensitivity of LC molecules as microdroplets. The response of LC microdroplets to interfacial forces is also found to vary with the type of polymers and surfactant used in their fabrication.^{42,47,53-56} Similar trends were observed in our recent studies on LC microdroplets system used for the detection of KB cancer cells.⁵⁶ Considering the studies reported in the literature, it has been hypothesized that the polystyrene segment of amphiphilic polymer has played a significant role in controlling the optical response in LC microdroplets on interaction with antigen at the interface. Studies reported in the literature clearly indicate that the orientational response of LC microdroplets could be used^{40-46,52} for a sensitive and label-free

detection of antigen in comparison LC molecules on solid surfaces^{33-36,47-48} and antibody-conjugated AuNPs.^{2,4} Therefore, in the present study, we attempted to develop a LC microdroplet-based biosensor for label-free detection of IgG using AIgG-anchored LC microdroplets in PBS solution. The response of LC microdroplets for the detection of IgG was also determined in 10% FBS and 10% blood plasma. LC microdroplets developed with different amounts of AIgG were used for the detection of IgG in PBS and other media and to optimize the amount of AIgG to control the sensitivity of LC microdroplets.

2. Experimental

2.1 Materials and methods

Poly(styrene-*b*-acrylic acid) (PS-*b*-PA) (Mw.: 7246 gmol⁻¹), 4-cyano-4'-pentyl biphenyl liquid crystal in 98% nematic phase (5CB) (Mw.: 249.15 gmol⁻¹, m.p.: 24°C), sodium dodecylsulfate (SDS) (Mw.: 288.38 gmol⁻¹), di-*tert*-butylpyrocarbonate, 1-ethyl-3-(3-dimethyl aminopropyl) carbodiimide hydrochloride (EDC) (Mw.: 312.38 gmol⁻¹), N-hydroxysuccinimide (NHS) (Mw.:115.09 gmol⁻¹), and fluorescein isothiocyanate (FITC) were purchased from Sigma-Aldrich Chemical Company, USA, and used as received. Phosphate-buffered saline solution (PBS) of pH 7.4 was used for washing and dispersion of LC microdroplets. The >95% pure reagent grade (SDS-PAGE) salt-free lyophilized white powder of rabbit antigen (IgG) (150 kDa) was purchased from Sigma-Aldrich Company, USA, and stored at < 8°C before using as reference antigen for immunoassaying of pathogens (viruses and bacteria) by LC microdroplets. Unconjugated rabbit anti-IgG (AIgG) (Mw.: 150 kDa, lyophilized white powder) was purchased from Sigma-Aldrich Company, USA. This AIgG is specific to rabbit IgG and does not react with human immunoglobulin-G (IgG). All measurements were carried out in PBS solution. Ultrapure water was prepared using Milli-Q system and used in all experiments. UV spectra were recorded

using double beam spectrophotometer using UV-vis spectrophotometer, Jasco-650, USA. The size distribution of LC microdroplets was determined using optical microscope (Nikon Eclipse TS100, Japan) and particle size analyzer (Beckman coulter, N/LS-1332, USA). Optical and polarized optical microscope images of LC microdroplets were recorded using Olympus IX 71 inverted fluorescence microscope using both cross-polarization and transmission modes. The upright fluorescence microscope (Olympus BX61, Olympus America Inc., USA) with fluorescent filter tube above objective lenses, coupled with a digital camera, was used for detection of FITC ($\lambda_{\text{EX}} = 519 \text{ nm}$). The AIGG- and FITC-AIGG-conjugates were synthesized by anchoring AIGG and FITC-AIGG to LC microdroplets.

2.2 Preparation of LC microdroplets

In order to prepare LC microdroplets, 10 mg (1.4 μmol) of block copolymers (PS-b-PA) were added to a 100 mL round bottom flask containing 10 mL PBS solution and 10 mg (35 μmol) of sodium dodecylsulfate (SDS). The mixture was magnetically stirred for about 30 min at 800 rpm for thorough mixing of SDS with amphiphilic block copolymer (PS-b-PA) to obtain a homogeneous mixture of PS-b-PA with SDS. Next, the LC microdroplets were prepared by dropwise addition of 10 ml PBS solution containing 50 mg (200 μmol) of 4-cyano-4'-pentyl biphenyl (5CB) liquid crystal (98% nematic phase) to the homogeneous solution of PS-b-PA and SDS. The resulting mixture was stirred continuously at 11,000 rpm for 1min for homogeneous dispersion of LC microdroplets. The emulsion consisting of dispersed LC microdroplets was centrifuged at 800 rpm in PBS solution (pH 7.4) to separate LC microdroplets from unused 5CB, SDS, and PS-b-PA. After removing supernatant containing small-sized microdroplets, the centrifuged LC microdroplets were dispersed in PBS solution and centrifuged again to collect size-selected samples of LC microdroplets. These LC microdroplets were preserved in PBS

solution for anchoring with AIgG in order to study their interactions with IgG in PBS and other media such as 10% FBS and 10% blood plasma. The size distribution of LC microdroplets was determined using optical microscope (Nikon Eclipse TS100, Japan) and particle size analyzer (Beckman coulter, N/LS-1332, USA). The orientational state of 5CB molecules in LC microdroplets was determined by recording optical and polarized optical microscope images using Olympus IX 71 inverted fluorescence microscope operating both cross-polarization and transmission modes. The bipolar and radial configuration of LC microdroplets was confirmed on the basis of their optical texture visible in optical micrographs recorded with Olympus IX 71 inverted fluorescence microscope. The optical images of LC microdroplets after interactions with IgG have shown two points of defects (boojums) indicating orientational transition from radial to bipolar. The bright field images of LC microdroplets after interaction with IgG have shown a bright spherical dot with dark dimples, confirming the transition from radial to bipolar. The orientation of 5CB molecules in LC microdroplets was found to be opposite to that reported by other workers.^{45,46,57} The application of small amount of SDS (51 μ mol) in fabrication of LC microdroplets has produced microdroplets with bipolar orientation⁴² in comparison to SDS (17.3 μ mol) used our studies which stabilized the LC molecules in radial configuration.

2.3 Conjugation of anti-IgG to LC microdroplets

The AIgG-anchored LC microdroplets were prepared by conjugating AIgG with activated carboxylic group of amphiphilic block copolymer in LC microdroplets. In order to activate the carboxylic group of amphiphilic block copolymer in LC microdroplets, 1.0 mL concentrate (9×10^3 microdroplets/mL) of LC microdroplets was added to a round bottom flask containing 10 mL PBS. To this solution, 100 mg (320 μ mol) of NHS and 100 mg (870 μ mol) of EDC was added and the solution was incubated for 1 h at room temperature in dark. Next, 5 μ g (34 pmol)

AIgG was added and after 12 h, the mixture was dialyzed using regenerated cellulose nitrate membranes to remove unused EDC, NHS, and other impurities. Finally, AIgG-anchored LC microdroplets were washed with PBS solution to remove unused AIgG. The amount of AIgG anchored on LC microdroplets was determined by Bradford method by using calibration curve drawn at $\lambda_{\max} = 278$ nm for different amounts of AIgG in PBS solution. The configuration of 5CB in LC microdroplets, before and after conjugation of AIgG, was determined by polarized optical microscopic examination of 1.0 mL PBS solution of AIgG-anchored LC microdroplets in a 1.0 cm diameter dish. The LC microdroplets were also prepared by varying the amounts of AIgG from 10 to 100 μg per 10 mL (6.8-68 pmol) in PBS solution containing 9×10^3 LC microdroplets to optimize the amount of AIgG for sensitive LC microdroplets for the detection of IgG.

2.4 Synthesis of FITC- and anti-IgG-anchored LC microdroplets

In order to confirm the presence of anti-IgG (AIgG) in LC microdroplets, AIgG was firstly conjugated with FITC and used to anchor to LC microdroplets. For conjugation of FITC with AIgG, 5 μg (34 pmol) of AIgG was added to a 10 mL solution of PBS containing 100 mg each of EDC and NHS. The solution was kept for 1 h at 5°C to activate the carboxylic group of the antibody. A freshly prepared 10 mL volume of DMSO solution containing 50 μg of FITC was added gently to this solution and left for 8 h in dark at 5°C. The reaction mixture was dialyzed using regenerated cellulose acetate membranes and FITC-conjugated AIgG was washed with PBS solution and lyophilized to obtain a powdery white solid. To anchor the FITC-conjugated AIgG on LC microdroplet, 10 mL PBS solution containing 25 μg FITC-conjugated AIgG was added to a 100 mL round bottom flask containing 1.0 mL LC microdroplets (9×10^3 microdroplets/mL), activating agents (EDC and NHS, 100 mg each), and 10 mL PBS solution.

The mixture of FITC-conjugated AIgG and LC microdroplets was incubated for 8h at 5°C. Then solution was dialyzed in PBS solution using regenerated cellulose membrane. Finally, LC microdroplets were preserved after washing with PBS solution to remove unused FITC-conjugated AIgG. In order to confirm the conjugation of FITC with AIgG, the UV spectra of FITC, AIgG, and FITC-conjugated AIgG were recorded using UV-vis spectrophotometer. The upright fluorescence microscope (Olympus BX61, Olympus America Inc., USA) with fluorescent filter tube above the objective lenses, coupled with a digital camera, was used to record the micrographs ($\lambda_{\text{EX}} = 519 \text{ nm}$) of FITC- and AIgG antibody-conjugated LC microdroplets. The optical and polarized optical microscope images of LC microdroplets with and without FITC-coupled AIgG were recorded using Olympus IX 71 inverted fluorescence microscope, operating both cross-polarization and transmission modes, to confirm the anchoring effect of AIgG and FITC-AIgG conjugates on the orientational state of 5CB molecules in LC microdroplets. The micrographs were recorded using 1.0 mL solution of LC microdroplets (9×10^3 microdroplets/mL) with and without FITC-conjugated AIgG in a optical dish of 1.0 cm diameter in PBS solution, to enable the microdroplets to move freely and prevent overlapping in the optical path during recording of micrographs. All experiments were performed in triplicates, and optical and polarized optical images were recorded at three different locations of the optical dish containing LC microdroplets.

2.5 Detection of rabbit-IgG using anti-IgG-anchored LC microdroplets

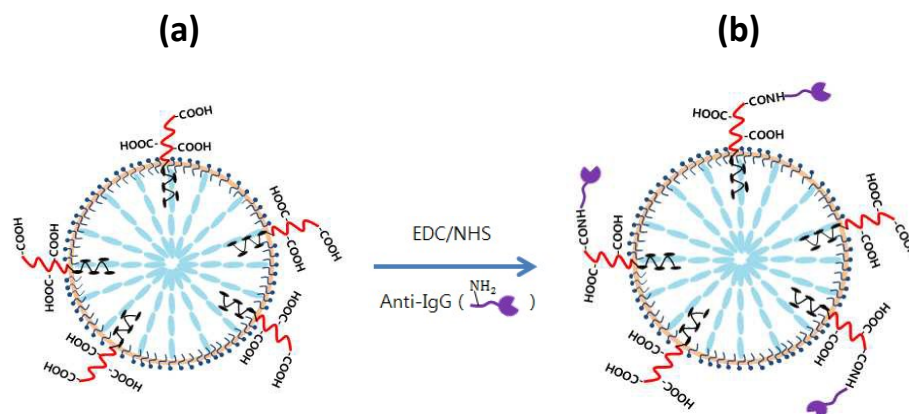
In order to measure the orientational variation of 5CB molecules in anti-IgG (AIgG)-anchored LC microdroplets for the detection of IgG, fixed amounts of pristine and AIgG-anchored LC microdroplets were incubated by varying the amount of IgG from 0 to 1000 ng/mL in PBS and in other media such as 10% FBS and 10% blood plasma. In order to determine the response time of

AIgG-conjugated LC microdroplets, the AIgG-conjugated LC microdroplets were incubated for different time-periods ranging from 30 to 90 min in PBS solution containing known amount of IgG. After incubation, polarized optical microscope images were recorded to visualize the effect of IgG interactions on the orientational state of 5CB molecules in LC microdroplets. The orientational variation in 5CB molecules in LC microdroplets was used to evaluate the response time. The sensitivity, lower detection limit and reproducibility of the optical response of LC microdroplets in detection of IgG were determined by carrying out experiments in triplicates. The orientational response of LC microdroplets with different amount of AIgG is evaluated to fabricate the LC microdroplets with high sensitivity and lower limit of detection of IgG in the solution. In different set of experiments, the orientational response of LC microdroplets was recorded in presence of 10% blood plasma to analyze the effects of other proteins such as blood human globulins (IgG, IgA, IgM, etc.) in detection of IgG by AIgG-anchored LC microdroplets.

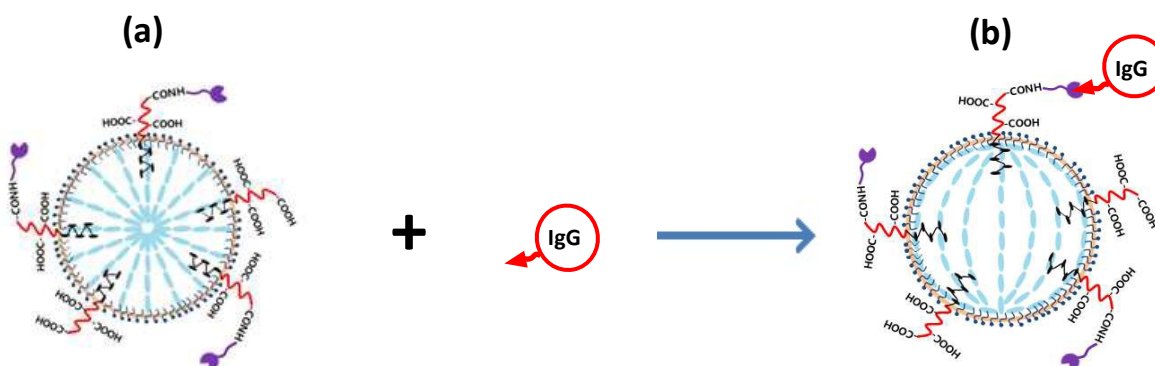
3. Results and discussion

The development of a rapid and reliable method for detection of antibody and antigen in human blood serum is expected to be useful in diagnosis of diseases using infected blood samples.⁵⁸ Detection of antibody and its assaying found to be redundant in differentiating the past and present infections or in assessing the efficacy of treatments. This problem may be circumvented by detecting antigen and assaying method.⁵⁹ Several studies have indicated that immunoassaying of antigen is more useful for diagnosis of diseases than assaying the antibodies.⁶⁰⁻⁶¹ Various diagnostic approaches based on fluorescence immunoassaying using nanoparticles or quantum dots anchored with dye-labeled antibodies have been reported for the detection of antigens and tumor cells.^{21,22} In these studies it has been demonstrated that NP-based imaging probes emit a strong fluorescence signal, thus providing improved detection sensitivity

for clinical applications. In order to achieve antigen-specific targeting and emission of strong fluorescence for clinical applications, the fluorescent nanoparticles must be modified with high affinity targeting moieties. The surface of fluorescent nanoparticles needs to be modified appropriately in order to increase the stability and half-life of NPs in blood circulation. In view of these limitations of immunofluorescent-NPs, the AIgG-anchored LC microdroplets were prepared for sensitive and rapid detection of IgG in blood serum by recording optical signals of 5CB molecules in AIgG-anchored LC microdroplets. The goat AIgG is a secondary antibody with strong affinity for binding the heavy chains of rabbit IgG. In order to enhance the sensitivity of 5CB in detection of interfacial interactions, 5CB was used in the form of LC microdroplets⁴⁰⁻⁴⁶ to enable the achievement of an optically detectable response in the presence of virus and bacteria. The small-sized 5CB droplets provided more surface area and sensitivity, similar to the nanoparticles-based assaying methods.⁶²⁻⁶³ The force of interfacial interactions in the presence of minimal amounts of IgG (< 20 ng/mL) was sufficient to produce detectable optical signals by 5CB in LC microdroplets; however, 5CB on solid planar surface produces optically detectable signals in the presence of microgram amounts of analytes.^{34,35,64} This indicated that 5CB in the form of microdroplets is more sensitive to interfacial events and interactions than 5CB on solid planar surfaces. The LC microdroplets and AIgG-anchored LC microdroplets showed radial configuration (Scheme 1) but AIgG-anchored LC microdroplets were only successful in showing orientational variation on interaction with IgG (Scheme 2). As pristine LC microdroplets were not able to interact strongly with IgG, orientational variation from radial to bipolar was visible in AIgG-anchored LC microdroplets in PBS (pH 7.4) solution and other media (Scheme 2). The change in configurational transition in LC microdroplets on interaction with IgG provides the basis for real-time and sensitive detection of IgG in biological fluids.



Scheme 1. Orientational state of 5CB in LC microdroplets before (a) and after (b) anchoring AIGG.



Scheme 2. Orientational state of 5CB in AIGG-anchored LC microdroplets before (a) and after (b) interactions with IgG.

3.1 Synthesis of FITC- and anti-IgG-anchored LC microdroplets

In order to confer target-specific binding affinity to LC microdroplets, the AIGG- anchored LC microdroplets were prepared using amphiphilic block copolymer (PS-*b*-PA) and 5CB in the presence of SDS surfactant by the method reported in our earlier communication.⁵⁶ The anchoring of AIGG is carried out using a fraction of LC microdroplets of sizes varying from 20 to 30 μm . The absorbance ($\lambda_{\text{max}} = 278 \text{ nm}$) of mixture of filtrate and LC microdroplets

washings was determined by Bradford method (Fig. 1) to find out the amount of AIgG anchored on LC microdroplets.

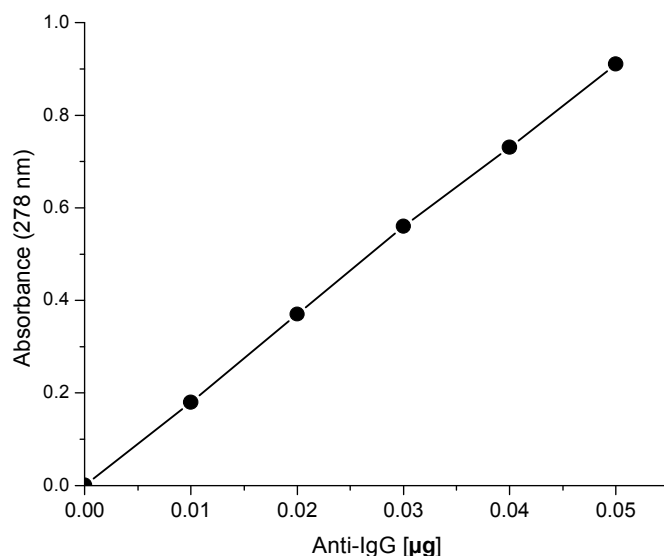


Figure 1. Calibration curve for quantitation of AIgG.

The AIgG-anchored LC microdroplets within the size range of 20–30 μm have produced naked eye-visible signals in polar micrographs on interaction with IgG. These were not observed for the AIgG-anchored LC microdroplets whose size was lower than 10 μm . However, the configurational state of 5CB in LC microdroplets was similar to that in the LC microdroplets of size 20–30 μm . The configuration of 5CB in LC microdroplets was confirmed by recording polar micrographs using polarized optical microscopy. These results indicate that 5CB molecules are stabilized in radial configuration in the LC microdroplets, due to the dynamic nanostructure of amphiphilic block copolymer and SDS surfactant at the interface and in the core of the microdroplets. The styrenic benzene of amphiphilic block copolymer was found to control the orientation of 5CB molecules in the core of LC microdroplets, while polar and hydrophobic alkyl

parts of SDS controlled the interactions of 5CB at the interface and within the bulk of the LC microdroplets. The 1:5 weight ratio of SDS and amphiphilic block copolymer employed was able to stabilize 5CB in radial configuration in LC microdroplets ranging from 10 to 30 μm in size in PBS (pH 7.4) solution.

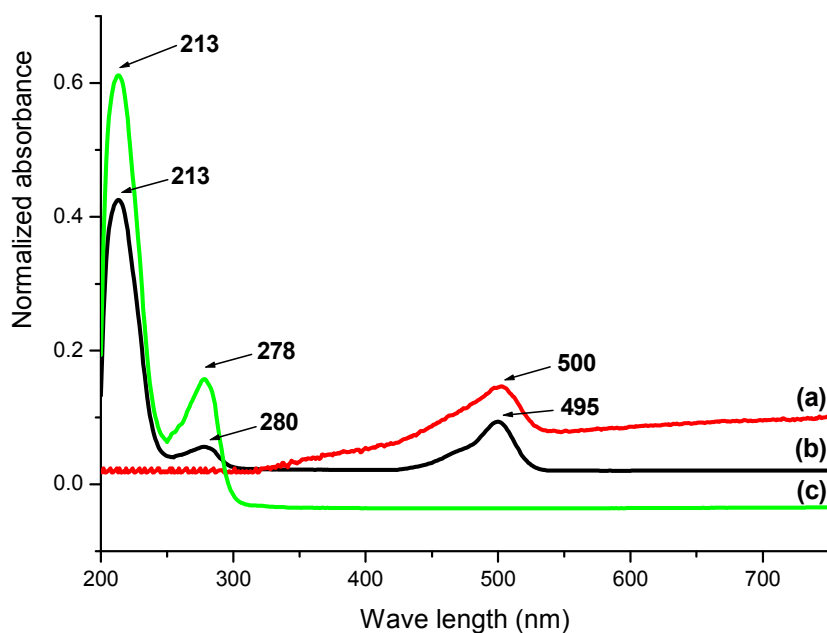


Figure 2. UV-spectra of FITC (a), FITC-conjugated AIGG (b), and AIGG (c).

The presence of an absorption band at 495 nm in the UV spectrum of FITC-conjugated AIGG (Fig. 2b) confirmed the conjugation of FITC (Fig. 2a) with AIGG (Fig. 2c). The UV spectrum of pure FITC showed a characteristic band⁶⁵ at 500 nm (Fig. 2a). Pure AIGG did not show an absorption band at around 500 nm (Fig. 2c). The fabricated FITC-conjugated AIGG was subsequently used to anchor to LC microdroplets using activating agents EDC and NHS (100 mg each) in PBS solution at 5⁰C. In order to confirm the presence of AIGG on LC microdroplets, fluorescence images of LC microdroplets anchored with FITC-AIGG conjugate were recorded

using fluorescence microscopy. The presence of green fluorescence of LC microdroplets confirmed the anchoring of AIgG to LC microdroplets (Fig. 3).

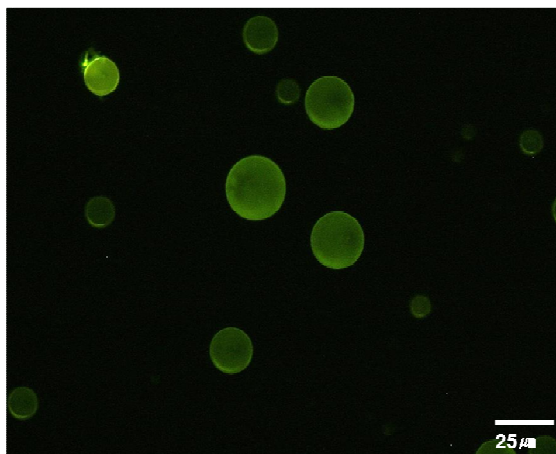


Figure 3. Fluorescence image of FITC-AIgG-anchored LC microdroplets.

The fluorescence images of LC microdroplets anchored with FITC-AIgG conjugate also confirmed the average size variation of LC microdroplets (10–30 μm) in the samples (Fig. 3). The anchoring of AIgG to LC microdroplets (Scheme 2) did not elicit a change in the configurational state of 5CB in the microdroplets. In order to confirm the configurational state of 5CB in LC microdroplets, the polarized optical micrograph of LC microdroplets without AIgG (Fig. 4a) was compared with the polarized optical micrograph showing LC microdroplets anchored with AIgG (Fig. 4b). The comparison between polarized optical micrographs of LC microdroplets with and without AIgG (Fig. 4) clearly indicates that LC microdroplets with and without AIgG both showed 5CB in radial state. This suggested that the anchoring of AIgG on LC microdroplets did not influence the interactions of SDS and amphiphilic block copolymer with

5CB molecules in the core of LC microdroplets, which may be due to the presence of weak interaction forces between AIgG and LC microdroplets.

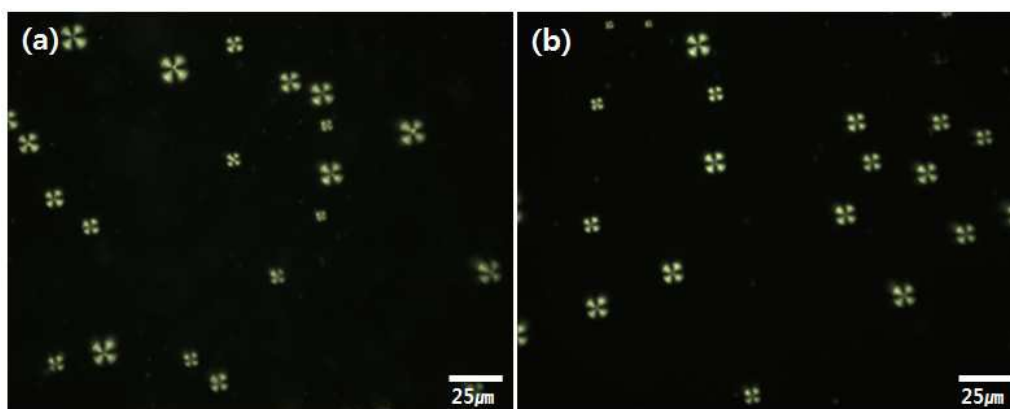


Figure 4. Polarized optical microscope images of LC microdroplets before anchoring of AIgG (a) and after anchoring of AIgG/FITC-AIgG conjugates (b).

The anchoring of AIgG to LC microdroplets produces symmetrical and weak interaction forces around the 5CB molecules, which were not sufficient to polarize the orientation of these molecules in the LC microdroplets. Therefore, no configurational transition in 5CB molecules was observed to occur in LC microdroplets on anchoring of AIgG. This further indicates that AIgG anchors symmetrically to LC microdroplets without creating any local field to polarize the 5CB molecules. LC microdroplets with fixed surface density of AIgG were obtained by optimizing the amount of AIgG. To this end, different amounts of AIgG were used with fixed density of LC microdroplets (9×10^3 microdroplets/mL) at sufficient amount of IgG (1000 ng/mL) and the optical signals were recorded. The response of LC microdroplets has shown variation on varying the anchoring amount of AIgG from 1–10 $\mu\text{g/mL}$ (6.8–68 pmol) on 9×10^3 LC microdroplets/mL. Each LC microdroplet conjugated with 3.33×10^{-3} pmol of AIgG has shown high sensitivity than conjugated with low ($< 3.33 \times 10^{-3}$ pmol) or high ($> 3.33 \times 10^{-3}$ pmol)

amount of AIgG. These results indicated that 5 $\mu\text{g/mL}$ (34 pmol) of AIgG was sufficient to form IgG sensitive monolayer (3.33×10^{-3} pmol of AIgG) around each microdroplets on conjugating with 9×10^3 LC microdroplets/mL. At low amount of AIgG (1 $\mu\text{g/mL}$, 6.8 pmol), the IgG sensitive layer of AIgG was formed a small fraction LC microdroplet to transmit the interfacial forces to the core of LC microdroplets to induce configurational transition in 5CB molecules, whereas on taking more amount of AIgG (10 $\mu\text{g/mL}$, 68 pmol), a thick layer of coiled chains of AIgG is formed, which was less sensitive to interact with IgG and interaction force was insufficient to induce configurational transition in all LC microdroplets. The fraction of LC microdroplets with sensitive monolayer of AIgG (3.33×10^{-3} pmol/LC microdroplet) was reduced on conjugating with high amount of AIgG (10 $\mu\text{g/mL}$, 68 pmol) in comparison to LC microdroplets obtained at 5 $\mu\text{g/mL}$ (34 pmol) of AIgG. However, the fraction of LC microdroplets with sensitive layer of AIgG (3.33×10^{-3} pmol/microdroplet) was high in comparison to LC microdroplets conjugated with 1 $\mu\text{g/mL}$ (6.8 pmol) of AIgG. The LC microdroplets anchored with 5 $\mu\text{g/mL}$ of AIgG have shown configurational transition in 5CB molecules in large fraction of LC microdroplets (9×10^3 microdroplets/mL) in the presence of 1000 ng/mL concentration of IgG, indicating that 5 $\mu\text{g/mL}$ of AIgG was adequate to form a uniform sensitive layer on a large fraction of LC microdroplets, as examined using polarized optical microscope. This is confirmed from the polarized optical micrograph recorded on incubating LC microdroplets anchored with 5 $\mu\text{g/mL}$ of AIgG in PBS solution containing 1000 ng/mL of IgG (Fig. 1Sb) and from LC microdroplets with low amount of AIgG ($< 5 \mu\text{g/mL}$) recorded with 50 ng/mL of IgG (Fig. 7a & b).

3.2 Sensitivity evaluation of anti-IgG-anchored LC microdroplets in detection of IgG

In order to avoid interference from FITC in the detection of IgG using configurational variation in 5CB molecules in LC microdroplets, the AIGG-anchored LC microdroplets were used for immunoassaying of IgG in PBS and other media such as 10% FBS, and 10% blood plasma. A calculated volume of AIGG-anchored LC microdroplets concentrate was added to an optical dish (1.0 cm diameter) to achieve a constant density of LC microdroplets (9×10^3 microdroplets/mL) for recording the configuration variation in LC microdroplets in presence of IgG. The response of LC microdroplets to the presence of IgG was studied by varying the concentration of IgG from 20 to 1000 ng/mL. The diffusional and dilution effect on interactions of IgG with AIGG-anchored LC microdroplets was avoided by maintaining the final volume of LC microdroplets and IgG at 1.0 mL. In order to avoid the effect of temperature on the interactions between IgG and LC microdroplets, the incubation dishes containing AIGG-anchored LC microdroplets and IgG were maintained at room temperature and allowed to shake horizontally to provide enhanced opportunity for interaction between IgG and AIGG-anchored LC microdroplets. After incubation for 30 min, the configurational state of 5CB in AIGG-anchored LC microdroplets was examined by recording polarized optical micrographs at 3 or 4 different locations of the optical dish in order to obtain an average view of the orientational variation of 5CB in LC microdroplets. All experiments were recorded in triplicates to ensure reproducibility. The polarized optical images of LC microdroplets incubated for 30 min in PBS solution (pH 7.4) indicated that LC microdroplets incubated with 10 ng/mL of IgG, like the original LC microdroplets, showed radial configuration (Fig. 5a & Fig. 4). The LC microdroplets incubated with 20 ng/mL of IgG showed clear configurational variation from radial to bipolar (Fig. 5b). It was observed that, on further increasing the amount of IgG to more than 20 ng/mL, the fraction of LC microdroplets showing bipolar configuration increased significantly at 50 ng/mL concentration of IgG.

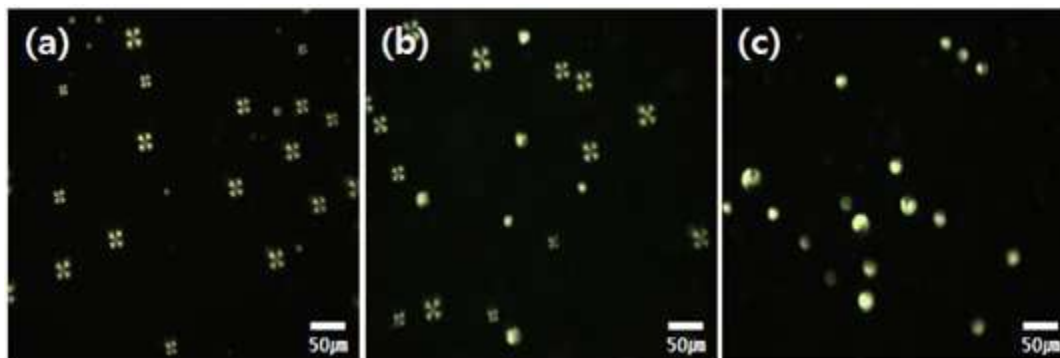


Figure 5. Polarized optical microscope images of AIGG-anchored LC microdroplets incubated in PBS (pH 7.4) having different concentration of IgG at a constant density of LC microdroplets (9×10^3 microdroplets/mL) anchored with $5 \mu\text{g/mL}$ of AIGG. Contact time: 30 min. Temp.= room temperature, [IgG] = (a) 10 ng/mL, (b) 20 ng/mL, (c) 50 ng/mL.

The increase in number of LC microdroplets with bipolar configuration has continued till 800 ng/mL amount of IgG in test solution. This increasing trend was attributable to the increased rate of diffusion of IgG from bulk phase of the test solution to the surface of LC microdroplets, where it was able to bind with AIGG anchored to the LC microdroplets. The fraction of LC microdroplets with bipolar configuration has continued to increase on increasing the amount of IgG till 800 ng/mL while keeping other variables constant. The LC microdroplets have shown high sensitivity in transforming LC microdroplets from radial to bipolar (2.5 LC microdroplets/ng of IgG) within the concentration range of IgG from 20-800 ng/mL (Table 1). On further increasing the amount of IgG (> 800 ng/mL), the LC microdroplets have shown a decreasing trend in their sensitivity (< 2.5 LC microdroplets/ng of IgG), which might be due to the increase in viscosity of the medium (Fig.1Sa). On incubating LC microdroplets loaded with $5 \mu\text{g/mL}$ of AIGG in a solution with ≥ 1000 ng/mL IgG, the sensitivity of LC microdroplets has decreased as a significant fraction of LC microdroplets remained with bipolar orientation (Fig 1Sb). This has supported that prepared LC microdroplets were useful for the detection of IgG

within the concentration range from 20-800 ng/mL. No variation in orientational state of 5CB in LC microdroplets was observed on further increasing the amount of IgG beyond 1000 ng/mL, which might be due to significant reduction in interactions of IgG with AIgG anchored-LC microdroplets. This result demonstrates correlation between the fraction of LC microdroplets showing configurational transition and the amount of IgG used to interact with AIgG-anchored LC microdroplets upto a maximum amount of 1000 ng/mL of IgG in test solution. This correlation has been found to be useful for determining the lower limit of detection of IgG by LC microdroplets. The lower limit of detection of LC microdroplets anchored with 5 μ g/mL (34 pmol) of AIgG was found to be 16 ng/mL of IgG for a concentration range of IgG from 20 to 800 ng/mL in PBS (pH 7.4). The LC microdroplets anchored with 10 μ g/mL (68 pmol) of AIgG have shown low sensitivity (< 2.0 LC microdroplets/ng of IgG) but upper detection limit was enhanced to 940 ng/mL and lower limit of detection of IgG was found to be same as with LC microdroplets anchored with 5 μ g/mL (34 pmol) of AIgG (Table 1). The LC microdroplets anchored with 1 μ g/mL (6.8 pmol) of AIgG were found to be less sensitive (0.8 LC microdroplets /ng of IgG) in transforming LC microdroplets with radial configuration to bipolar configuration on interaction of IgG in test solution. The working range for detection of IgG was found to be 80-560 ng/mL and lower limit of detection for IgG was > 60 ng/mL (Table 1).

Table 1. Performance of AIgG-anchored LC microdroplets in detection of IgG.

AIgG (μ g/mL)	Sensitivity for IgG (LCdroplets/ng)	Working range (ng/mL of IgG)	LOD (ng/mL)	Reproducibility (%)
1.0	0.8	80-560	60	3-8
5.0	2.5	20-800	16	1-6
10.0	1.8	20-940	16	2-10

The lower detection limit of LC microdroplets anchored with optimized amount of AIGG (5 μ g/mL) for the detection of the antigen found to be within the limit reported by other methods. The conventional ELISA is time consuming and able to show LOD 8ng/mL for the detection of antigen whereas electrochemical ELISA⁶⁶ shown LOD of 0.3 ng/mL. The electrochemical ELISA needs sufficient time in sample preparation and to generate detectable signal in comparison to LC molecules based biosensor. The fluorescent immunoassaying of malarial antigen in infected human blood by AuNP based system⁴ has shown a LOD of 2.4 μ g/mL, which is quite high in comparison to LOD of IgG (16ng/mL) found in present investigation. The LC microdroplet detection of IgG has also been found better in comparison to recent studies based on microfluidic LC based system for the detection of antigen (1 μ g/mL).⁵² The results indicate that the application of 5CB as LC microdroplets provides the advantage of sensitive detection of IgG in nano-range in comparison to 5CB on solid surface^{64,65} and other detection systems.^{67,68} The high sensitivity of the LC microdroplets developed in the present study is attributable to their small size (20–30 μ m) in comparison to larger-sized LC microdroplets (60–85 μ m) used for the detection of proteins.⁶⁵ In order to analyze the effect of proteins on orientational variation in 5CB in LC microdroplets, the response of AIGG-anchored LC microdroplets containing 5 μ g of AIGG was studied in other media such as 10% FBS and 10% blood plasma, for fixed amounts of IgG (20 ng/mL).

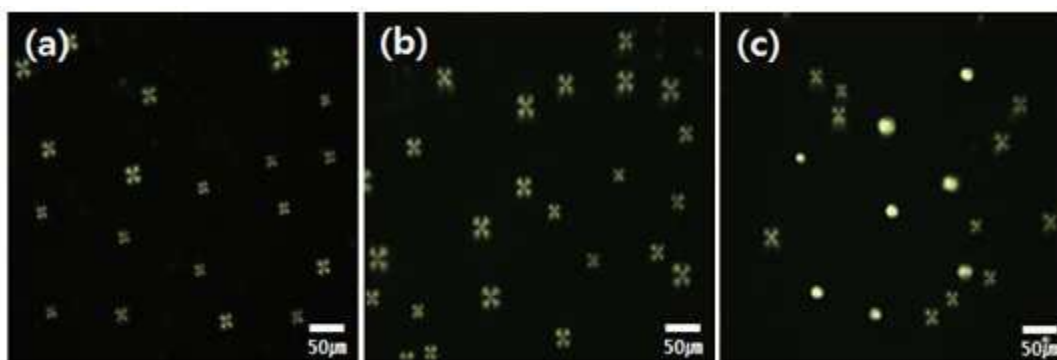


Figure 6. Polarized optical microscope images of LC microdroplets for the detection of IgG in 10% FBS, recorded at different contact times, at constant density of LC microdroplets (9×10^3 microdroplets/mL) using 20 ng/mL concentration of IgG test solution at room temperature. Contact time: 30 min (a), 60 min (b), and 90 min (c).

The polarized optical micrographs of LC microdroplets incubated with 20 ng/mL concentration of IgG in 10% FBS at contact times of 30 min and 60 min were found to be similar to those of the AIgG anchored LC microdroplets without IgG (Fig. 6a, b). However, on further increasing the contact time to 90 min, the polarized optical micrographs showed sufficient LC microdroplets with bipolar configuration (Fig. 6c). The AIgG anchored LC microdroplets were also used in 10% blood plasma for the detection of IgG. Corresponding micrographs were recorded (Fig. 7) at different time intervals, as with 10% FBS. The AIgG anchored LC microdroplets, which were in contact with IgG for 30 and 60 min in 10% blood plasma, showed radial configuration of 5CB molecules (Fig. 7 a & b). The configuration of LC microdroplets was same as observed for the original LC microdroplets in absence of IgG; however, on further increasing the contact time to 90 min, the 5CB molecules in LC microdroplets showed substantial number of LC microdroplets with bipolar configuration of 5CB (Fig. 7c).

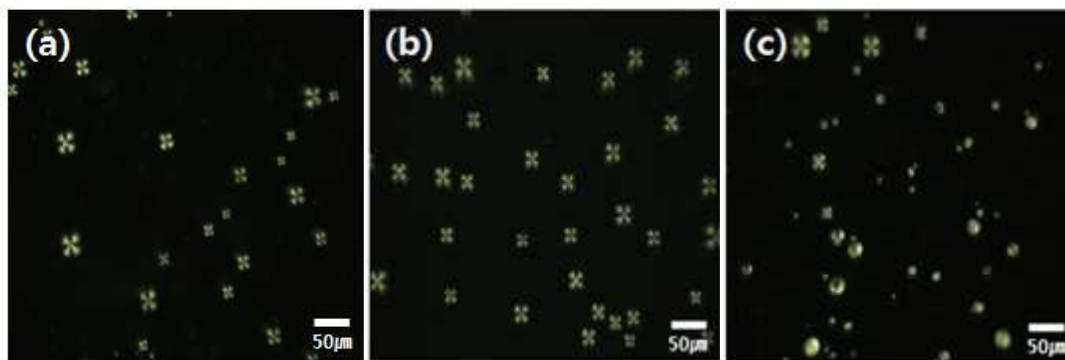


Figure 7. Polarized optical microscope images of LC microdroplets for the detection of IgG in 10% blood plasma, recorded at different contact times, at constant density of LC microdroplets (9×10^3 microdroplets/mL) using 20 ng/mL concentration of IgG in test solution at room temperature. Contact time: 30 min (a), 60 min (b), and 90 min (c).

The results of IgG interactions with AIgG anchored LC microdroplets in 10% FBS and 10% blood plasma indicate that AIgG-anchored microdroplets may be used for the detection of IgG in 10% FBS and 10% blood plasma. However, in order to obtain the same configurational variation in 5CB as in LC microdroplets obtained from PBS medium, the LC microdroplets in 10% FBS and 10% blood plasma must be allowed a contact time of 90 min. The presence of non-specific protein molecules in 10% FBS and 10% blood plasma has slowed down the rate of diffusion of IgG molecules to LC microdroplets and able to generate optimal signal at 90 minutes for detection of IgG (Fig. 2S).

3.3 Sensitivity evaluation of LC microdroplets fabricated with different amounts of anti-IgG

In order to evaluate the minimum amount of AIgG required for fabrication of the 5CB-based LC microdroplets sensor for the detection of IgG, 1.0 mL of LC microdroplets of constant density (9×10^3 microdroplets/mL) was used to anchor different amounts of AIgG in the presence of activating agents (EDC and NHS, 100 mg each). The LC microdroplets fabricated with different

amounts of AIgG were used to evaluate configurational response to a fix amount of IgG (50 ng/mL) in PBS for a contact time of 30 min at 30°C. The amounts of AIgG used to anchor to a 9×10^3 microdroplets/mL concentration of LC microdroplets varied from 1.0-10 $\mu\text{g/mL}$ (6.8-68 pmol). The resulting mixture was incubated with IgG (50 ng/mL) for a contact time of 30 min in PBS solution. After incubation, the configurational state of 5CB in LC microdroplets was examined by recording polarized optical micrographs in optical dish of 1.0 cm diameter (Fig. 8). The polarized optical micrograph of LC microdroplets anchored with 1.0 $\mu\text{g/mL}$ (6.8 pmol) amount of AIgG indicated radial configuration of 5CB without any change in orientation from radial to bipolar in any of the LC microdroplets (Fig. 8a). However, a substantial fraction of the LC microdroplets anchored with 5 $\mu\text{g/mL}$ (34 pmol) of AIgG showed bipolar orientation (Fig. 8b).

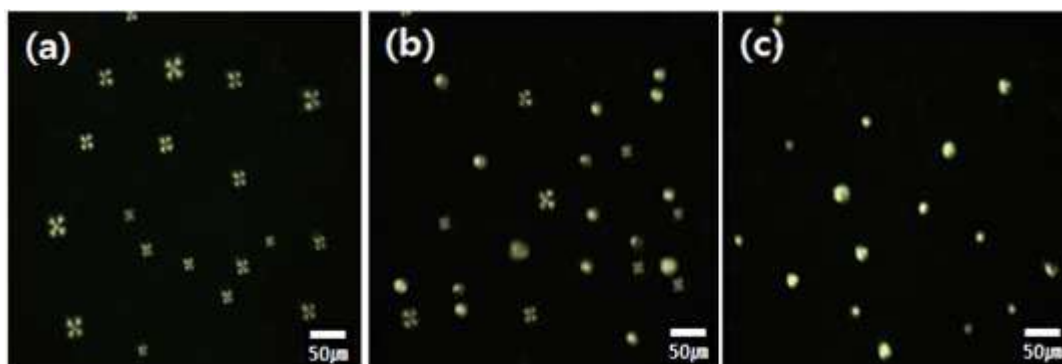


Figure 8 Polarized optical microscope images of LC microdroplets fabricated with different amount of AIgG. The configurational variation in AIgG-anchored LC in PBS (pH = 7.4) at 50 ng/mL of IgG. Temp. = room temperature, contact time: 30 min. [AIgG] = 1.0 $\mu\text{g/mL}$ (a), 5.0 $\mu\text{g/mL}$ (b) and 10.0 $\mu\text{g/mL}$ (c).

The number of LC microdroplets with bipolar configuration increased further for LC microdroplets anchored with more amounts of AIgG ($> 5 \mu\text{g/mL}$). The LC microdroplets anchored with 10 $\mu\text{g/mL}$ (68 pmol) of AIgG showed maximum configurational transition from radial to bipolar (Fig. 8c). The force of interactions between IgG and LC microdroplets anchored

with 5.0 $\mu\text{g/mL}$ (34 pmol) of AIgG was sufficient to induce detectable orientational variation in LC microdroplets with optimal surface density of AIgG (3.33×10^{-3} pmol / microdroplet). On further increasing the amount of AIgG ($> 5.0 \mu\text{g/mL}$), the number of LC microdroplets with the optimal amount of AIgG increased but overall sensitivity was found to decrease due to the presence of sufficient number of LC microdroplets possessing a thick layer of AIgG (Table 1). Accordingly, the fraction of LC microdroplets with bipolar configuration increased significantly on anchoring LC microdroplets with 10 $\mu\text{g/mL}$ (68 pmol) of AIgG (Fig. 7c) but these LC microdroplets shown less sensitivity for IgG as shown in Table 1. The orientational variation of LC microdroplets with different amounts of AIgG was also recorded in 10% FBS and 10% blood plasma in presence of 50 ng/mL concentration of IgG. The trends in variation in orientational configuration for LC microdroplets fabricated with different concentrations of AIgG at 50 ng/mL concentration of IgG in 10% FBS and 10% blood plasma were similar to those of PBS solution. However, the fraction of LC microdroplets with bipolar configuration was found to be slightly lower in comparison to LC microdroplets in PBS solution. These findings clearly demonstrate that LC microdroplets anchored with 5.0 $\mu\text{g/mL}$ (6.8 pmol) of AIgG were having high sensitivity (2.5 ± 0.01 LC microdroplets/ng of IgG) for the detection of IgG in PBS and other media such as 10% FBS and 10% blood plasma within a concentration range of 20-1000 ng/mL of IgG with a response time of 30 min at room temperature. The sensitivity and working range for detection of IgG has shown significant variation on varying the amount of AIgG anchored on LC microdroplets (Table 1).

3.4. Validation of IgG detection by AIgG anchored LC Microdroplets

To authenticate the accuracy in detection of IgG by AIgG anchored LC microdroplets, the IgG was detected in rabbit serum and percentage recovery of IgG was recorded from spiked sample

containing 25 ng/mL of IgG. The calibration curve drawn between numbers of LC microdroplets Vs concentration of IgG was used to determine the amount of IgG in rabbit serum and percent recovery of IgG in spiked sample. The detection of IgG was carried out in triplicates to validate the accuracy and precision of IgG detection by LC microdroplets in PBS. The amount of IgG in rabbit serum was found to be 68 ng/mL ($\pm 4\%$), which is almost comparable within the range of IgG found in rabbit serum. The percent recovery and coefficient of variance for spiked sample were found to be 106% and $\pm 6\%$ respectively for a spiked amount of 25 ng/mL of IgG in test sample.

4. CONCLUSIONS

In the present study, we successfully demonstrated that the orientational response of liquid crystal molecules might be utilized for developing a sensitive and label-free biosensor for the detection of pathogenic proteins in biological fluids. Our results also indicate that the sensitivity of LC microdroplets for the detection of protein may be improved further by controlling the size of the LC microdroplets and controlling the surface density of antibody on these microdroplets. The LC microdroplets prepared were stable in PBS solution at pH 7.4 and were able to detect IgG with great precision and accuracy. We are attempting to extend these findings to the development of a dual detection system to confirm the selectivity and sensitivity of LC microdroplets for the detection of proteins. To this end, we aim to utilize the immunofluorescence and orientational variation of 5CB in LC microdroplets on interaction with nano-amounts of proteins in solution. The technique should enable non-invasive detection of cancer-specific biomarkers in biological fluids such as blood and urine, with great sensitivity.

AUTHOR INFORMATION

Corresponding Author

Prof. Inn-Kyu Kang
Department of Polymer Science and Engineering, Kyungpook National University,
Daegu 702-701, South Korea.
Tel: + 82 53 950 5629
Fax: + 82 53 950 6623
Email: ikkang@knu.ac.kr

Co-Corresponding Author

Email: kcgptfcy@iitr.ac.in (Prof. KC Gupta)

NOTES

The authors declare no competing financial interests.

ACKNOWLEDGMENTS

One of the authors, Prof. K.C. Gupta, is thankful to Prof. Inn-Kyu Kang for carrying out collaborative research as Visiting Professor at his Laboratory in South Korea under KOFST program (131S-2-3-05630). This research was supported by the Basic Research Laboratory Program (No 2011-0020264) and General Research Program (2013 RIAIA 2005148) of the Ministry of Education, Science and Technology of Korea.

REFERENCES

1. M. Hawkes, K.C. Kaim, Advances in malaria diagnosis, *Expert Rev Anti-infect Ther.*, 2007, **5**, 485-495.
2. The mal ERACGoD, Diagnostics, A research agenda for malaria eradication: diagnoses and diagnostics, *PLoS Med*, 2011, **8**, e1000396.
3. T. Kreising, R. Hoffmann, and T. Zuchner, Novel time-resolved fluorophores for protein detection, *Anal. Chem.*, 2011, **83**, 4281-4287.

4. B.S. Guirgis, C. Sá e Cunha, I. Gomes, M. Cavadas, I. Silva, G. Doria, G.L. Blatch, P.V. Baptista, E. Pereira, H.M. Azzazy, M. M. Mota, M. Prudêncio, R. Franco, Gold nanoparticle-based fluorescence immunoassay for malaria antigen detection, *Anal Bioanal Chem.*, 2012, **402**, 1019-1027.
5. S.R. Inglis, M. Strieker, A.M. Rydzik, A. Dessen, and C.J Schofield, A boronic-acid-based probe for fluorescence polarization assays with penicillin binding proteins and β -lactamases, *Anal. Biochem.*, 2012, **420**, 41-47.
6. R. Arai, H. Nakagawa, K. Tsumoto, W. Mahoney, I. Kumagai, H. Ueda, and T. Nagamuni, Demonstration of a homogeneous noncompetitive immunoassay based on bioluminescence resonance energy transfer, *Anal. Biochem.*, 2001, **289**, 77-81.
7. Z. Altintas, Y. Uludag, Y. Gurbuz, and I.E.Tothill, Surface plasmon resonance based immunosensor for the detection of the cancer biomarker carcinoembryonic antigen, *Talanta*, 2011, **86**, 377-383.
8. B. Du, Z. Li, and Y.Cheng, Homogeneous immunoassay based on aggregation of antibody-functionalized gold nanoparticles coupled with light scattering detection, *Talanta*, 2008, **75**, 959-964.
9. D.I.Stott, Immunoblotting and dot blotting, *J. Immuno methods*, 1989, **119**, 153-187.
10. P. Baptista, E. Pereira, P. Eaton, D. Doria, A.A. Miranda, I. Gomes, P. Quaresma, and R. Franco, Gold nanoparticles for the development of clinical diagnosis methods , *Anal. Bioanal Chem.*, 2008, **391**, 943-950.
11. Xinag Cui, Mei Liu and Baoxin Li, homogeneous fluorescent based immunoassay via inner effect of gold nanoparticles on fluorescence of CdTe quantum dots, *Analyst*, 2012, **137**, 3293-3299.

12. J.-M. Nam, C.S Thaxton, and C.A. Mirkin, Nanoparticle- based bio-bar codes for the ultrasensitive detection of proteins, *Science*, 2003, **301**, 1884-1886.
13. S. Pathak, S.K. Choi, N. Arnheim, and M.E. Thompson, Hydroxylated quantum dots as luminescent probes for in situ hybridization, *J. Am. Chem. Soc.*, 2001, **123**, 4103-4104.
14. X. Wu, H. Liu, J.Liu, K.N. Haley, J.A. Treadway, J.P. Larson, N. Ge, F. Peale, and M.P. Bruchez, Immunofluorescent labeling of cancer marker Her2 and other cellular targets with semiconductor quantum dots, *Nat. Biotechnol.*, 2002, **21**, 41-46.
15. X. Gao, Y. Cui, R.M. Levenson, L.W.K. Chung, and S. Nie, In vivo cancer targeting and imaging with semiconductor quantum dots, *Nat. Biotechnol.*, 2004, **22**, 969- 976.
16. T.A. Taton, C.A. Mirkin, and R.L. Letsinger, Scanometric DNA array detection with nanoparticle probes, *Science*, 2000, **289**, 1757-1760.
17. L. Zhu, S. Ang, W.-T. Liu, Quantum dots as a novel immunofluorescent detection system for cryptosporidium parvum and Giardia lamblia, *Appl. Environ. Microbiol.*, 2004, **70**, 597-598.
18. X. J. Zhao, L.R. Hillard, S. J. Mechery, Y.P. Wang, R. P. Wagwe, S.G. Jin, and W. H. Tan, A rapid bioassay for single bacterial cell quantitation using bio-conjugated nanoparticles, *Proc. Nat. Acad. Sci. USA*, 2004, **101**, 15027-15032.
19. S. Dwarakanath, J. G. Bruno, A. Shastry, T. Phillips, A. A. John, A. John, A. Kumar, L.D. Stephenson, Quantum dot-antibody and aptamer conjugates shift fluorescence upon binding bacteria, *Biochemical and Biophysical Research Communications*, 2004, **325**, 739-43.
20. S. Jiang, Y. Zhang, K.M.Lim, E.K.Sim, L. Ye, NIR-to-visible upconversion nanoparticles for fluorescent labeling and targeted delivery of siRNA, *Nanotechnology*, 2009, **20**, 155101-155110.

21. Yildiz Uludag, Güzin Köktürk, Determination of prostate-specific antigen in serum samples using gold nanoparticle based amplification and lab-on-a-chip based amperometric detection, *Microchimica Acta*, 2015, **182**, 1685-1691.
22. M. De, S. Rana, H. Apnikar, O.R. Miranda, R. R. Arvizo, U. H. F. Bunz, and V.M. Rotello, Sensing of proteins in human serum using conjugates of nanoparticles and green fluorescent protein, *Nature Chemistry*, 2009, **1**, 461 - 465.
23. H. Tan, X. Li, S. Liao, R. Yu, Z. Wu, Highly-sensitive liquid crystal biosensor based on DNA dendrimers-mediated optical reorientation, *Biosens. Bioelectron.*, 2014, **62**, 84-89.
24. S. Yang, C. Wu, H. Tan, Y. Wu, S. Liao, Z. Wu, G. Shen, and R. Yu, Label-Free Liquid Crystal Biosensor Based on Specific Oligonucleotide Probes for Heavy Metal Ions, *Anal. Chem.*, 2012, **85**, 14-18.
25. H. Tan, S. Yang, G. Shen, R. Yu, and Z. Wu, Signal enhanced liquid crystal DNA biosensors based on enzymatic metal deposition, *Angew. Chem.*, 2010, **122**, 8790-8793.
26. F. Zuo, Z. Liao, C. Zhao, Z. Qin, X. Li, C. Zhang, D. Liu, An air-supported liquid crystal system for real-time reporting of host-guest inclusion events, *Chem. Commun.*, 2014, **50**, 1857-1860.
27. M.L. Bungabong, P.B. Ong, K.-L. Yang, Using copper perchlorate doped liquid crystals for the detection of organophosphate vapor, *Sens. Actuator B: Chemical*, 2010, **148**, 420-426.
28. D. Hartono, S.L. Lai, K. L.-L. Yang, L.Y.L. Yung, A liquid crystal-based sensor for real-time and label-free identification of phospholipase-like toxins and their inhibitors, *Biosens. Bioelectron.*, 2009, **24**, 2289-2293.

29. H. J. VanTreeck, D.R. Most, B.A. Grinwald, K.A. Kupcho, A. Sen, M.D. Bond, and B.R. Acharaya, Quantitative detection of a simulant of organophosphate chemical warfare agents using liquid crystals, *Sens. Actuators B: Chemical*, 2011, **158**, 104-110.
30. H. Xu, X. Bi, X. Ngo, K.-L. Yang, Principles of detecting vaporous thiols using liquid crystals and metal ion microarrays, *Analyst*, 2009, **134**, 911-915.
31. X. Bi, K.-L. Yang, Real-time liquid crystal-based glutaraldehyde Sensor, *Sens. Actuators B: Chemical*, 2008, **134**, 432-437.
32. S. Sivakumar, K.-L. Yang, J. K. Gupta, N.L. Abbott, and F. Caruso, Liquid crystal emulsions as the basis of biological sensors for the optical detection of bacteria and viruses, *Adv. Funct. Mater.*, 2009, **19**, 2260-2265.
33. C.-Y. Xue, K.-L. Yang, Dark-to-bright optical responses of liquid crystals supported on solid surfaces decorated with proteins, *Langmuir*, 2008, **24**, 563-567.
34. C.-S. Xue, S.A. Khan, K.-L. Yang, Exploring optical properties of liquid crystals for developing label-free and high-throughput microfluidic immunoassays, *Adv. Funct. Mater.*, 2008, **21**, 198-202.
35. L. Birchall, R. Ulijn, S. Webb, A combined SPS-LCD sensor for screening protease specificity, *Chem. Commun.*, 2008, 2861-2863.
36. D. Hartono, W.J. Qin, K.-L. Yang, L.Y.L Yung, The effect of cholesterol on protein-coated gold nanoparticle binding to liquid crystal-supported models of cell membranes, *Biomaterials*, 2009, **30**, 843-849.
37. X. Bi, K.-L. Yang, Liquid crystals decorated with linear oligopeptide FLAG for applications in immunobiosensors, *Biosens. Bioelectron.*, 2010, **26**, 107-111.

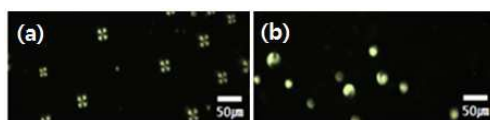
38. X. Bi, D. Hartono, K.-L. Yang, Real-time liquid crystal pH sensor for monitoring enzymatic activities of penicillinase, *Adv. Funct. Mater.*, 2009, **19**, 3760-3765.
39. V. J. Alino, J. Pang, and K.-L. Yang, Liquid crystal droplets as a hosting and sensing platform for developing immunoassays, *Langmuir*, 2011, **27**, 11784-11789.
40. N.A. Lockwood, J. K. Gupta, N. L. Abbott, Self-assembly of amphiphiles, polymers and proteins at interfaces between thermotropic liquid crystals and aqueous phases, *Suf.Sci.Rep.*, 2008, **63**, 255-293.
41. S. Sivakumar, K. L. Wark, J. K. Gupta, N. L. Abbott, F. Caruso, Liquid crystal emulsions as the basis of biological sensors for the optical detection of bacteria and viruses, *Adv. Funct. Mater.*, 2009, **19**, 2260-2265.
42. O. Tongcher, R. Siegel, K. Landfester, Liquid crystal nanoparticles prepared as miniemulsions, *Langmuir*, 2006, **22**, 4504-4511.
43. K.A. Simon, P. Sejwal, R.B. Gerecht, Y.-Y. Luk, Water-in-water emulsions stabilized by non-amphiphilic interactions: Polymer-dispersed lyotropic liquid crystals, *Langmuir*, 2007, **23**, 1453-1458.
44. E. Tjipto, K.D. Cadwell, J.F. Quinn, A.P. Johnson, N.L. Abbott, F. Caruso, Tailoring the interfaces between nematic liquid crystal emulsions and aqueous phases via layer-by-layer assembly, *Nano Lett.*, 2006, 2243-2248.
45. J. K. Gupta, S. Sivakumar, F. Caruso, N.L. Abbott, Size-dependent ordering of liquid crystals observed in polymeric capsules with micrometer and smaller diameters, *Angew. Chem. Int. Ed.*, 2009, **121**, 1680-1683.
46. S. Sivakumar, J.K. Gupta, N.L. Abbott, F. Caruso, Monodisperse emulsions through templating polyelectrolyte multilayer capsules, *Chem. Mater.*, 2008, **20**, 2063-2065.

47. J.K. Gupta, J.S. Zimmerman, J.J. de Pablo, F. Caruso, and N.L. Abbott, Characterization of adsorbate-induced ordering transitions of liquid crystals within monodisperse droplets, *Langmuir*, 2009, **25**, 9016-9024.
48. I.H. Lin, D.S. Miller, P.J. Bertics, C.S. Murphy, J.J. dePablo and N.L. Abbott, Endotoxin-induced structural transformations in liquid crystalline droplets, *Science*, 2011, **332**, 1297-1300.
49. T. Bera and J. Y. Fang, Optical detection of lithocholic acid with liquid crystal emulsions, *Langmuir*, 2013, **29**, 387–390.
50. Y. Choi, K. Lee, K. C. Gupta, S. Y. Park and I.K. Kang, The role of ligand–receptor interactions in visual detection of HepG2 cells using a liquid crystal microdroplet-based biosensor, *J. Mater. Chem. B*, 2015, **3**, 8659-8969.
51. D. Wang, S.Y. Park, I. K. Kang, Liquid crystals: emerging materials for use in real-time detection applications, *J. Materials Chemistry C: Materials for Optical and Electronic Devices*, 2015, **3**, 9038-9047.
52. Q. Zhu, Y.-L. Yang, Microfluidic immunoassay with plug-in liquid crystal for optical detection of antibody, *Analytica. Chimica. Acta.*, 2015, **853**, 696-701.
53. L. Tortora, and O. D. Lavrentovich, Chiral symmetry breaking by spatial confinement in tactoidal droplets of lyotropic chromonic liquid crystals, *Proc. Natl. Acad. Sci. USA*, 2011, **108**, 5163-5168.
54. R. J. Carlton, Y.M. Zayas-Gonzalez, U. Manna, D.M. Lynn, and N.L. Abbott, Surfactant-induced ordering and wetting transitions of droplets of thermotropic liquid crystals “Caged” inside partially-filled polymeric capsules, *Langmuir*, 2014, **30**, 14944-14953.

55. J. H. Zou, T. Bera, A.A. Davis, W. L. Liang, and J.Y. Fang, Director Configuration transitions of polyelectrolyte coated liquid-crystal droplets, *J. Phys. Chem. B*, 2011, **115**, 8970-8974.
56. S.H. Yoon, K.C. Gupta, J. S.Borah, S.Y. Park, Y.K. Kim, J.H. Lee, and I.K. Kang, Folate ligand anchored liquid crystal microdroplets emulsion for in vitro detection of KB cancer cells, *Langmuir*, 2014, **30**, 10668–10677.
57. E. Tjipto, K. D. Cadwell, J.F. Quinn, A.P. Johnson, N.L. Abbott, F. Caruso, Tailoring the Interfaces between Nematic Liquid Crystal Emulsions and Aqueous Phases via Layer-by-Layer Assembly, *Nano Lett.*, 2006, 2243-2248.
58. P.T. Ravinder, S.C. Parija, K. S. Rao, Evaluation of human hydatid disease before and after surgery and chemotherapy by demonstration of hydatid antigens and antibodies in serum., *J. Med. Microbiol.*, 1997, **47**, 859-864.
59. O. Doiz, R. Benito, Y. Sbihi, A. Osuna, A. Clavel, R. Gomez-Lus, Western blot applied to the diagnosis and post-treatment monitoring of human hydatidosis, *Diagn. Microbiol. Infect Dis.*, 2001, **41**, 139-142.
60. D. Carmena, A. Benito, E. Eraso, Antigens for the immunodiagnosis of Echinococcus granulosus infection: an update, *Acta Trop.*, 2006, **98**, 74-86.
61. T. Sunita, M. L. Dubey, S. Khurana, N. Malla, Specific antibody detection in serum, urine and saliva samples for the diagnosis of cystic echinococcosis, *Acta Trop.*, 2007, **101**, 87-191.
62. A. Munir, J. Wang, H.S. Zhou, Dynamics of capturing process of multiple magnetic nanoparticles in a flow through microfluidic bioseparation system, *Let Nanobiotechnology*, 2009, **3**, 55-64.

63. K. S. Kim, J. K. Park, Magnetic force-based multiplexed immunoassay using superparamagnetic nanoparticles, *Lab on a Chip*, 2005, **5**, 657-664.
64. C.Y.Xue, K.-L. Park, Dark-to-bright optical responses of liquid crystals supported on solid surfaces decorated with proteins, *Langmuir*, 2008, **24**, 2008, 563-567.
65. V. J. Alino, J. Pang, K.-L. Yang, Liquid crystal droplets as a hosting and sensing platform for developing immunoassay, *Langmuir*, 2001, **27**, 11784-11789.
66. A.C. Glavan, D.C. Christodouleas, B. Mashadegh, H. D. Yu, B.S. Smith, J. Lesing, M.T. Fernandes-Abedul, and G.M. whitesides, Folding analytical devices for electrochemical ELISA in hydrophobic PH paper, *Anal. Chem.*, 2014, **86**, 11999-12007.
67. H. J. Kim, K. C. Ahn, A. Gonzalez-Techera, G.G. Gonzalez-Sapienza, S.J. Gee, B.D. Hammock, Magnetic bead-based phage anti-immunocomplex assay (PHAIA) for the detection of the urinary biomarker 3-phenoxybenzoic acid to assess human exposure to pyrethroid insecticides, *Analytical Biochemistry*, 2009, **386**, 45-52.
68. T. Franke, L. Schmid, D.A. Weitz, A. Wixforth, Magneto-mechanical mixing and manipulation of picoliter volumes in vesicles, *Lab on a Chip*, 2009, **9**, 2831–2835.

Table of content



AlG anchored LC microdroplets showing configurational transition from radial (a) to bipolar (b) on interaction with IgG.